

Precise simulation of thermal effects in side diode-pumped laser slab

M. H. MOGHTADER DINDARLU*, GH. SOLOOKINEJAD, H. IZADNESHAN, M. JABBARI^a, M. NAFAR^a

Department of Physics, Marvdasht branch, Islamic Azad University, Marvdasht, Iran

^aDepartment of Electronic Engineering, Marvdasht branch, Islamic Azad University, Marvdasht, Iran

In this paper, a precise simulation is performed for thermal effects of the side diode-pumped laser slab by using ZEMAX and LASCAD programs. First, by considering all details of pumping structure such as number of laser diode bars, distances, their pump distribution and divergence angles, ray tracing and absorbed pump density into the slab are simulated by ZEMAX. Then, the absorbed pump data file, obtained from ZEMAX, is entered into LASCAD. The thermal effects are analyzed by defining of material parameters, slab dimensions, cooling conditions and meshing structure in this software. Simulation results include temperature and stress distribution (Two-dimensional and three-dimensional), deformation and focal length of thermal lens. To certify the value of the simulation, the thermal effects results of laser slab are compared for different pump powers and coefficients of force convection heat transfer.

(Received July 12, 2016; accepted November 25, 2016)

Keywords: Temperature distribution, Stress distribution, Laser slab, Diode-pumping, Ray tracing

1. Introduction

In high-power solid state laser, the temperature of laser crystal is increased because of absorbed pump power [1,2]. Due to the temperature gradient created in the crystal, mechanical stresses occur in it. Temperature gradient and stress result in a change in the refractive index and thus the thermal effects such as thermal lens and induced birefringence occur in laser crystal [3-8]. Since these effects can decrease the output power and beam quality of laser output, precise knowledge of them is necessary [2,9-12]. There are usually two ways to determine the thermal effects of laser crystal; namely, analytical models and simulations. The former are provided depending on different factors such as crystal geometry (cylindrical or rectangular geometry), pump structure (for example, end-pumping or side-pumping) and type of cooling (conduction or convection) [13-19]. In all of these models, a distribution (for example, Gaussian profile) should be considered for absorbed pump power in the laser crystal that is an approximation. Therefore, the results of these models cannot be very careful and real. The latter are usually performed by software based on the Finite Element Method (FEM). For example, by using ANSYS and LASCAD programs, temperature and stress distributions can be simulated in crystals of solid state lasers [20]. Changes in the curvature of the crystal surfaces and focal length of thermal lens can also be calculated by LASCAD software. However, in this software, a distribution (for example, Gaussian or top-hat profile) for absorbed pump power must be considered. This means that we cannot directly enter the details of the pumping structure in the software.

In this paper, the details of the pump cavity are considered and all of them are simulated by ZEMAX

software. These details include the location of each laser diode, their distances from each other, type of their pump distribution, their pump powers, their divergence angles in fast and slow axes and the distance between the laser diodes and laser crystal. Thus, tracing pump beams in the laser crystal is performed, and then the data file is entered into LASCAD software. By defining the conditions of cooling and meshing structure for laser crystal, the thermal effects are simulated by LASCAD. Therefore, according to the considerations, accurate and real simulations can be expected.

2. Simulations

We want to simulate thermal effects of a side diode-pumped Nd:YAG laser slab (with doping concentration of 1.1%). Dimensions of laser slab are $12.5 \times 6 \times 130$ mm. Laser diode stack used for pumping has a width of 10 mm and contains 48 diode bars whose distance from each other is 2 mm. This stack is located at a distance of 3 mm from pump face of slab. Distribution of output radiation of laser diodes is as Gaussian profile. Their divergence angles have been considered 7 and 38 degrees in slow and fast axes, respectively (figure 1). Power of one diode bar is assumed 10 W so that the total power of diode stack will be 480 W. Slab is pumped from top face, and unabsorbed pump radiation is reflected from opposite face (bottom face). Fast axis of laser diodes is considered to be in direction of the slab width.

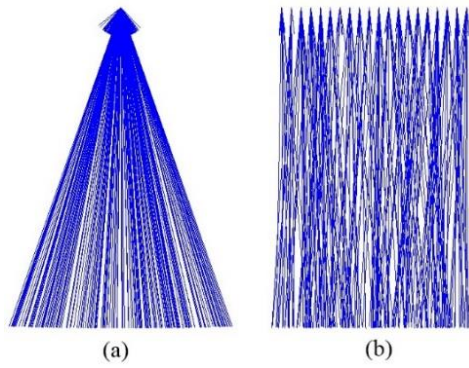


Fig. 1. Radiation of a laser diode bar, (a) fast axis, (b) slow axis

2.1. Simulation of ray tracing by ZEMAX

By considering the number of diodes, their distance from each other, their distance to pump face, their pump distribution, their divergence angles and optical power, the pump radiation transferred from the diode bars to the laser slab is modeled by the non-sequential mode of ZEMAX (see Fig. 2). The Nd:YAG material is entered as a new material in a custom glass catalog. Both the refractive and absorption properties are entered. A slab of Nd:YAG is collocated with a detector volume. This consists of $200 \times 200 \times 50 = 2000000$ voxels. The detector volume records the absorbed flux in each volume. The laser slab has a high-reflectivity coating on its bottom face (opposite face of pump face) so that un-absorbed light is reflected back into the laser slab. 48000000 rays have been traced, and the absorbed flux in the laser slab are measured.

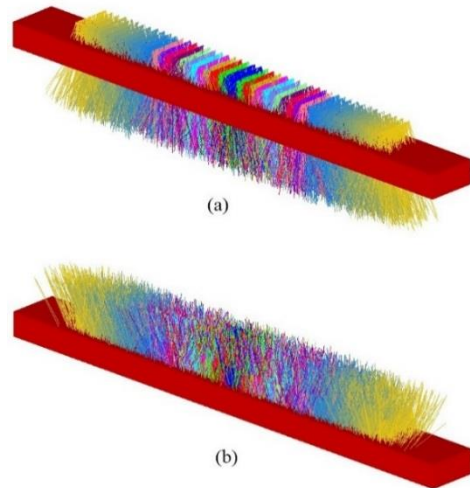
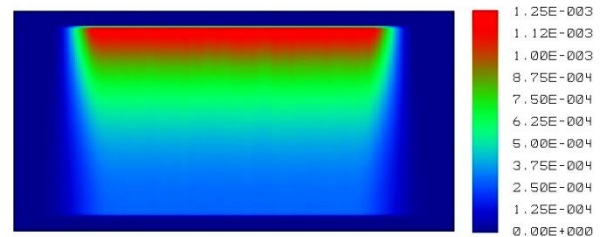
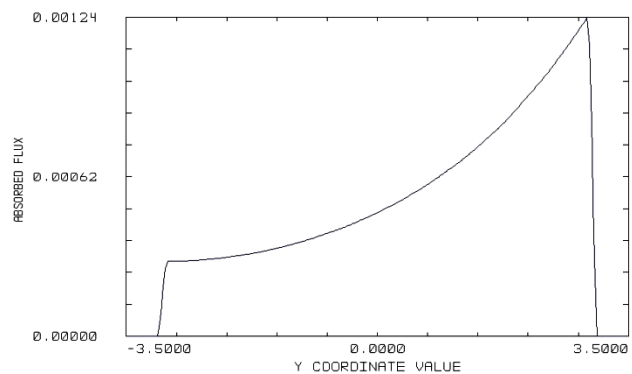
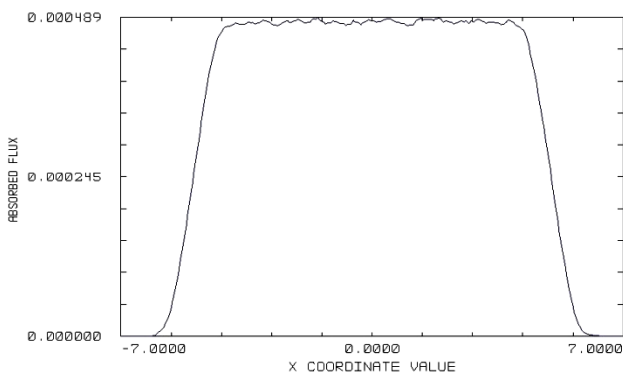


Fig. 2. Modeling a side diode-pumped laser slab in ZEMAX, (a) without and (b) with high-reflectivity coating of opposite face



DETECTOR IMAGE: ABSORBED FLUX
 THU JUN 16 2016
 DETECTOR 1, NSCG SURFACE 1:
 SIZE 14,000 W X 7,000 H X 156,000 L MILLIMETERS, PIXELS 200 W X 200 H X 50 L
 PEAK ABSORBED FLUX : 1.2497E-003 WATTS
 Z PLANE: 25 OF 50, Z : -1.560000E+000

Fig. 3. Absorbed flux and its data in cross-section of laser slab



THU JUN 16 2016
 DETECTOR 1, NSCG SURFACE 1: ROW CENTER, Y = 0.0000E+000
 SIZE 14,000 W X 7,000 H X 156,000 L MILLIMETERS, PIXELS 200 W X 200 H X 50 L
 PEAK ABSORBED FLUX : 1.2497E-003 WATTS
 Z PLANE: 25 OF 50, Z : -1.560000E+000

Fig. 4. 2D curve of absorbed flux in directions of (a) slab width and (b) slab thickness

The absorbed flux and its data in cross-section of laser slab are shown in figure 3. Moreover, 2D curve of absorbed flux in direction of x and y (width and thickness of laser slab) are shown in figures 4 (a,b). Fig. 4(a) related

to the absorbed flux in direction of the slab width is approximately similar to the top-hat profile.

The absorbed flux in direction of the slab thickness (Fig. 4(b)) is as the exponential curve. The absorption data

was exported as a text file for subsequent analysis by LASCAD.

2.2. Analysis of thermal effects by LASCAD

Finite Element Analysis (FEA) is used to compute temperature distribution, deformation, and stress or fracture mechanics in laser slab. The FEA code of LASCAD has been specifically applied to calculate thermal effects. Since the distribution of the absorbed pump power density has been computed by ZEMAX, data generated with this program can be used as input for LASCAD, which interpolates the 3D data set with respect to the grid used with the FEA code. Now, by specifying the dimensions of the laser slab, cooling conditions, material parameters and meshing structure, LASCAD software can be run. We consider water-cooling for the laser slab where its four-lateral faces are in contact with water of 20 degrees and its end faces are in contact with the surrounding air. The coefficient of force convection heat transfer with cooling water is assumed to be $0.01 \text{ Wmm}^{-2}\text{K}^{-1}$.

After completing calculations and simulations by LASCAD, the graphs of thermal effects such as the temperature and stress distributions, the pump absorbed distribution in directions of x and y and the deformation are available. 3D temperature distributions for the whole and half of the laser slab are shown in figure 5. According to this figure, the minimum and maximum temperatures of slab are 293 and 306.8 K, respectively. 2D temperature distributions in directions of width and thickness of slab (x and y axes, respectively) are shown in Fig. 6(a,b).

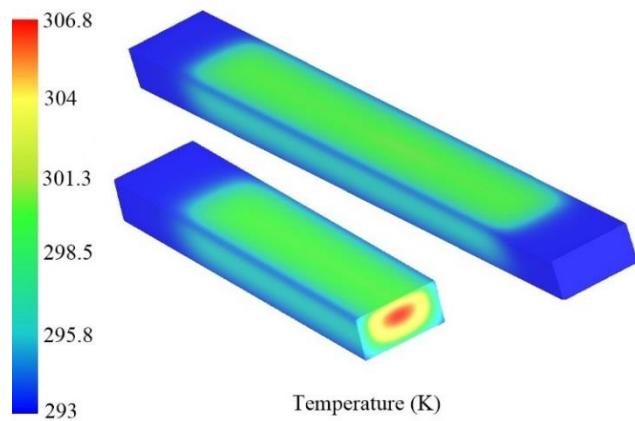


Fig. 5. 3D temperature distribution for the whole and half of the laser slab

According to Fig. 6(a,b), temperature distribution in direction of slab width (x-axis) is symmetric while it is asymmetric in direction of slab thickness (y-axis). It can be because the laser slab is pumped from one face. Different components of stress are also available. Here, only results of x-component are introduced. Three-dimensional distribution of this component is shown in Fig. 7. According to this figure, the minimum and

maximum stress in x-direction are -8.43 and 19.76 N/mm^2 , respectively.

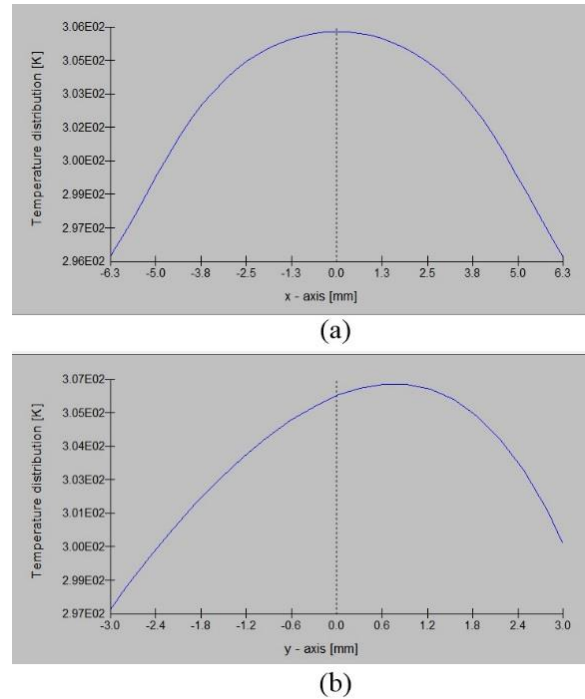


Fig. 6. 2D temperature distribution in directions of (a) slab width and (b) slab thickness

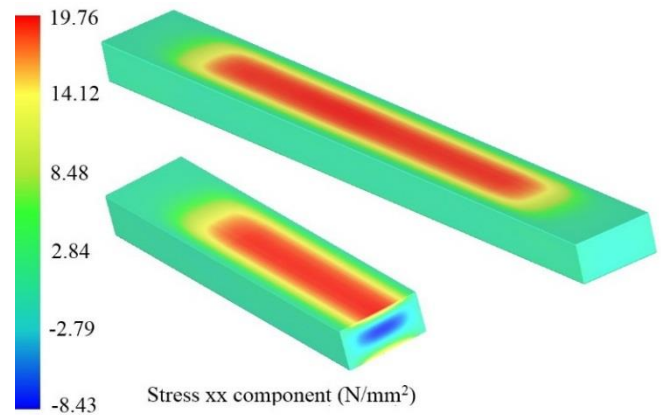


Fig. 7. 3D distribution of stress xx component for the whole and half of the laser slab

Fig. 8 shows the displacement y-component where its maximum value is in center of the pumped face (0.00025mm). LASCAD software also calculates the focal length of thermal lens. For this simulation, the focal length were obtained 788 and 2757 mm in y-z and x-z planes, respectively.

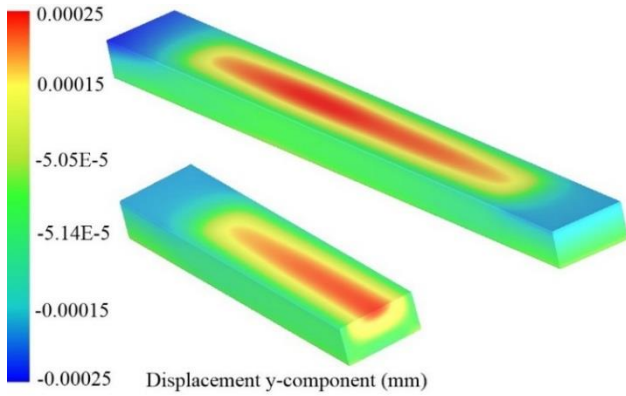


Fig. 8. 3D distribution of displacement y-component for the whole and half of the laser slab

To certify the value of the simulation, we compare the thermal effects results of laser slab for different pump powers and coefficients of force convection heat transfer. First, simulations are performed for different pump powers (240, 720 and 960W). The coefficient of force convection heat transfer is $0.01 \text{ Wmm}^{-2}\text{K}^{-1}$. According to the results of these simulations, maximum temperature, maximum stress in x-direction and maximum displacement y-component versus pump power have been plotted as shown in Fig. 9(a-c).

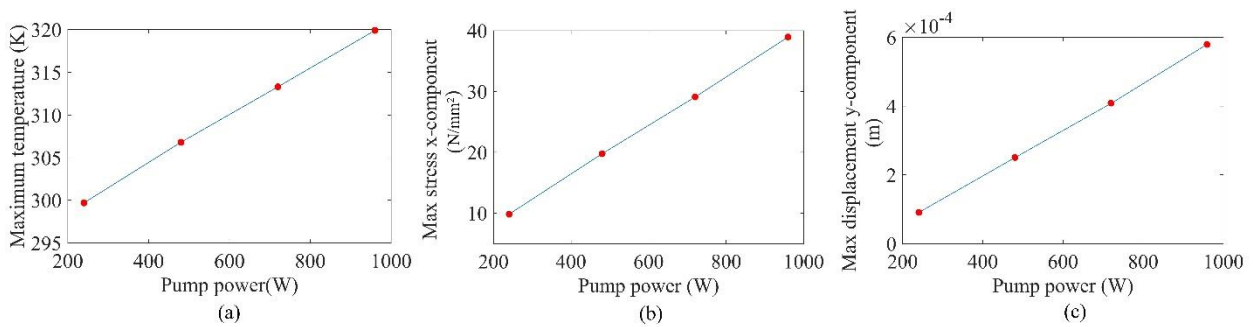


Fig. 9. Comparison of maximum temperature, stress x-component and displacement y-component in different pump powers

It is clear from the Fig. 9(a-c) that by increasing the pump power, the maximum temperature, stress x-components and displacement y-component will be increased because the heat generated in the laser slab is increased while the coefficient of heat transfer is constant (this increase is nearly linear).

Then, simulations are performed for pump power of 960W and different coefficients of force convection heat transfer ($0.005, 0.015, 0.02, 0.025, 0.03 \text{ Wmm}^{-2}\text{K}^{-1}$). According to the results of these simulations, maximum temperature, stress x-components and displacement y-component versus coefficients of force convection heat

transfer have been plotted as shown in Fig. 10(a-c). Fig. 10(a) shows that by improving cooling (i.e. increasing the heat transfer coefficient), the maximum temperature of laser slab is significantly reduced; so that by changing the coefficient of heat transfer from 0.005 to $0.03 \text{ Wmm}^{-2}\text{K}^{-1}$, temperature of laser slab will drop 17 degrees. According to Fig. 10(b), when the coefficient of heat transfer is increased the maximum stress x-component slightly rises. It is clear from Fig. 10(c) that by improving cooling, the maximum displacement y-component of laser slab is significantly reduced.

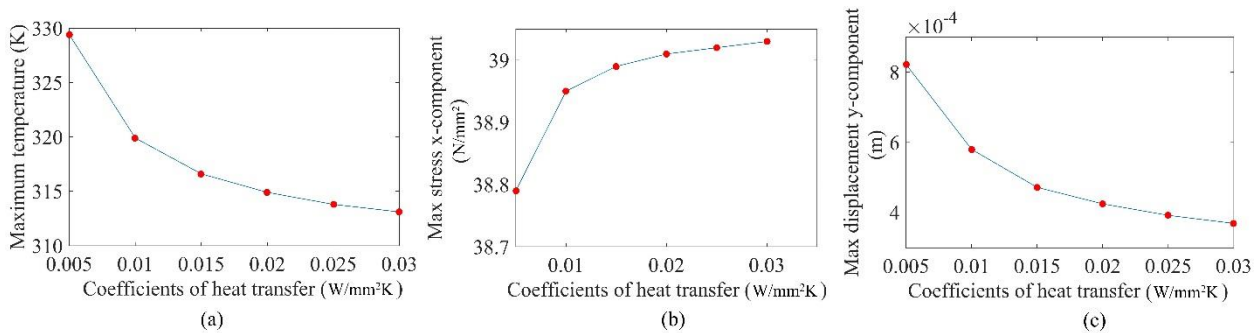


Fig. 10. Comparison of maximum temperature, stress x-component and displacement y-component in different coefficients of force convection heat transfer

Finally, the focal lengths simulated in y-z and x-z planes are compared for different pump powers as shown in Fig. 11. According to this figure, the focal length is decreased for larger pump power. This means that the

thermal lensing effect is magnified by increasing the pump power. This can be explained by using the Fig. 9(a,b). Since the greater stress and temperature gradient causes more severe changes in the refractive index of laser slab,

thermal lensing effect will become stronger (because the thermal lensing is caused by refractive index changes).

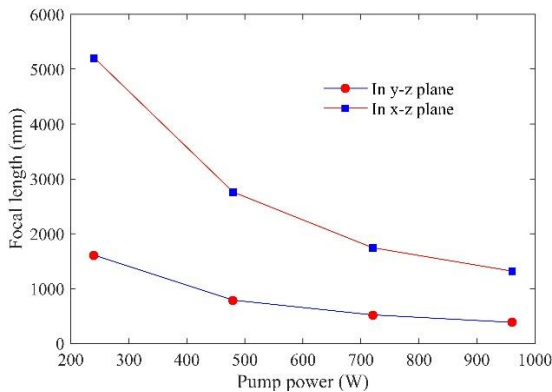


Fig. 11. The focal lengths in x-z and y-z planes for different pump powers

3. Conclusion

For a side diode-pumped laser slab, thermal effects such as temperature and stress distributions, deformation and focal length of thermal lens were simulated by ZEMAX and LASCAD programs. Since all details of pumping and cooling structure were considered, the simulation results can be trusted. All of the simulations were done for different pump powers and coefficient of heat transfer, and their simulation results were compared. This method can be used to simulate the thermal effects of other laser crystals with different pumping structures (for example, edge or end diode-pumped laser slabs, end or side diode-pumped laser rods). In addition, the laser crystals with flash-pumping structures can be simulated by method presented in this paper.

References

- [1] W. Koechner, Solid-state Laser Engineering (Berlin: Springer) 2006.
- [2] T. Y. Fan, IEEE J. Quantum Electron. **29**, 1457 (1993).
- [3] S. Fan, X. Zhang, Q. Wang, S. Li, S. Ding, F. Su,

- Opt. Commun. **266**, 620 (2006).
- [4] M. E. Innocenzi, H. T. Yura, C. L. Fincher, R. A. Fields, Appl. Phys. Lett. **56**, 1831 (1990).
- [5] I. Moshe, S. Jackel, A. Meir, Opt. Lett. **28**, 8 (2003).
- [6] I. Moshe, S. Jackel, J. Opt. Soc. Am. B. **22**, 1228 (2005).
- [7] M. S. Roth, E. W. Wyss, H. Glur, H. P. Weber, Opt. Lett. **30**, 1665 (2005).
- [8] G. He, J. Guo, B. Wang, Z. Jiao, Opt. Express. **19**, 18302 (2011).
- [9] J. D. Foster, L. M. Osterink, J. Appl. Phys. **41**, 3656 (1970).
- [10] Y. S. Huang, H. L. Tsai, F. L. Chang, Opt. Commun. **273**, 515 (2007).
- [11] J. Bourderionnet, A. Brignon, J. P. Huignard, R. Frey, Opt. Commun. **204** 299 (2002).
- [12] C. Liu, Laser Phys. **19**, 2155 (2009).
- [13] M. H. Moghtader Dindarlu, A. Maleki, H. Saghafifar, M. Kavosh Tehran, S. Baghali, Laser Phys. **25**, 045001 (2015)
- [14] M. H. Moghtader Dindarlu, M. Kavosh Tehrani, H. Saghafifar, A. Maleki, Chin. Phys. B **24**, 124205 (2015).
- [15] M. H. Moghtader Dindarlu, M. Kavosh Tehrani, H. Saghafifar, A. Maleki, Laser Phys. **26**, 055001 (2016).
- [16] A. Montmerle Bonnefois, M. Gilbert, P. Y. Thro, J. M. Weulersse, Opt. Commun. **259**, 223 (2006).
- [17] Z. Ma, D. Li, J. Gao, N. Wu, K. Du, Opt. Commun. **275**, 179 (2007).
- [18] P. Shi, W. Chen, L. Li, A. Gan, Appl. Opt. **46**, 4046 (2007).
- [19] M. Tilleman Michael, Optical Materials **33**, 363 (2011).
- [20] LAS-CAD, Laser Stability Analysis in LASCAD Software, the Unique Combination of Simulation Tools for Laser Cavity Analysis and Design, 2013, <http://www.lascad.com> Updated September 08

*Corresponding author: elsa27m@gmail.com